Energies **2014**, *7*, 874-889; doi:10.3390/en7020874

OPEN ACCESS

energies

ISSN 1996-1073

www.mdpi.com/journal/energies

Article

Modelling and Internal Fuzzy Model Power Control of a Francis Water Turbine

Klemen Nagode [1,*] and Igor Škrjanc [2]

[1] Department of Electrical Engineering, Sava Hydroelectric Power Plants Ljubljana d.o.o., Gorenjska Street 46, 1215 Medvode, Slovenia

[2] Department of System, Control and Cybernetics, Faculty of Electrical Engineering, Tržaška Street 25, SI-1000 Ljubljana, Slovenia; E-Mail: igor.skrjanc@fe.uni-lj.si

* Author to whom correspondence should be addressed; E-Mail: klemen.nagode@sel.si; Tel.: +386-1-4749-141; Fax: +386-1-4749-272.

Received: 17 November 2013; in revised form: 6 February 2014 / Accepted: 8 February 2014 / Published: 19 February 2014

Abstract: This paper presents dynamic modelling of a Francis turbine with a surge tank and the control of a hydro power plant (HPP). Non-linear and linear models include technical parameters and show high similarity to measurement data. Turbine power control with an internal model control (IMC) is proposed, based on a turbine fuzzy model. Considering appropriate control responses in the entire area of turbine power, the model parameters of the process are determined from a fuzzy model, which are further included in the internal model controller. The results are compared to a proportional-integral (PI) controller tuned with an integral absolute error (IAE) objective function, and show an improved response of internal model control.

Keywords: Francis turbine; fuzzy control; fuzzy model; hydro power plant; internal model control

1. Introduction

In HPPs, a digital turbine governor is an indispensable part of the control system. The stability of frequency, active power control, water flow control, turbine start-up procedure and emergency shut-down implemented with algorithms are major functions of digital turbine governor. Connected to Supervisory Control and Data Acquisition (SCADA), the unit controller, the excitation system and the

digital voltage controller, it enables the operator to change the operating states of generator, *i.e.*, the rotational speed, active power, reactive power and voltage.

With reference to achieving suitable control results and exploring the dynamic responses of a hydro power plant unit, it is necessary to obtain a mathematical hydraulic model of the hydro turbine and other parts of water system. Different types of hydraulic non-linear models were proposed in [1]: a non-linear model assuming a non-elastic water column, a model including travelling waves, and a model including a surge tank effect. In [2–7], the authors applied a non-linear or linearised model with a non-elastic water column to study the transient behaviour of a Francis turbine. Chen *et al.* provided a nonlinear dynamical model with surge tank presented with state space equations, analysed with bifurcation diagrams, phase orbits and spectrograms [8], however a comparison to the real system was neglected. In [9] authors developed interesting non-linear and linearised hydro turbine models with transient stability analysis in the free and open source Power System Analysis Toolbox (PSAT) software, although a conventional controller without a sophisticated tuning method was used.

Many recommendations of modelling, design and testing control systems for hydraulic turbines are described in international standards [10,11] and a few modern methods in [12,13], nevertheless in most cases a proportional-integral-derivative (PID) or proportional-integral (PI) controller is used for speed, active power, water level, flow and wicket gate opening control. However, the parameter determining process is usually taken on site acceptance tests; some recommendation limits are proposed in [11].

In [14] a particle swarm method was applied as a strategy in an improved gravitational search algorithm for identification of an optimal water turbine model and controller parameters. Fang *et al.* introduced the particle swarm optimization method of controller tuning in water turbine frequency control [15]. In [16] an internal model control (IMC) tuned PID controller in comparison with Ziegler-Nichols and singular frequency based tuning was studied for frequency control of hydropower system with a water hammer effect. The design of a PID controller based on sensitivity margin specifications was introduced in [17], where the author proposed the controller with respect to sensitivity peak specification. As a result in these cases, authors obtained optimal tuned PID parameters for water turbine control that could not necessarily result in optimal transient behaviour due to simplifications of the models and nonlinearity of real processes at different operating points.

In this paper, the focus is on mathematical modelling and the fuzzy power control approach of a Francis turbine of Aggregate 1 at hydro power plant (HPP) Moste. In the second section, the paper includes a comparison of non-linear and linearised models, with and without the surge tank of the Francis Turbine 1 in HPP Moste. In the third section, a fuzzy model of the Francis turbine has been applied based on a first order linearised model. Section 4 presents a fuzzy IMC controller with tuning parameter T to ensure a suitable dynamic response in working points and middle sections. At the end of Section 4, the comparison to the PI controller has been applied, tuned by the integral absolute error (IAE) objective function.

2. Non-Linear and Linearised Model of Turbine Dynamics

2.1. Description of the Hydro Power Plant

Slovenian hydro power production consists of three HPP chains placed on the Sava, Soca and Drava Rivers. As the first HPP on the Sava River chain with a unique accumulative operation type, HPP Moste plays an important role in the Slovenian hydro power plant generation portfolio.

HPP Moste is part of the HPP Moste and HPP Zavrsnica water system depicted in Figure 1. Besides 2,940,000 m^3 of useful volume of water storage, a −6.25 m water level deviation is allowed. After the water intake object, there is a surge tank connected by a tunnel. The pressure penstock connects the surge tank with a powerhouse, comprised of two Francis turbines (HPP Moste) and one Francis turbine (HPP Zavrsnica) with a joint tail-water conduit.

Figure 1. Hydro power plant (HPP) Moste and HPP Zavrsnica water system.

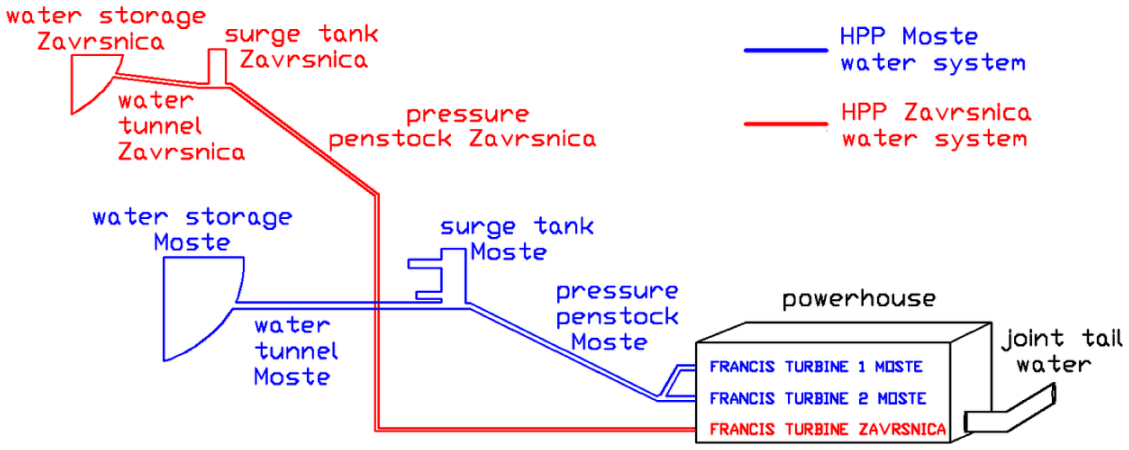

2.2. Turbine Model with Water Conduit

Turbine dynamics with the penstock are derived from second Newton's law [1,18] described with Equation (1):

$$\frac{d\bar{q}}{dt} = (\bar{h}_0 - \bar{h} - \bar{h}_f - \bar{h}_{sp}) \cdot g \cdot \frac{A}{l} \tag{1}$$

where $\bar{q}$ is turbine flow rate in m^3/s, with the penstock area section A in m^2 and length l in m. In Equation (1), $\bar{h}_0$ is the static head of the water column; $\bar{h}$ is the head at the turbine admission; $\bar{h}_f$ is defined as friction head loss; $\bar{h}_{sp}$ is the tail water head loss in m units and g is the gravity acceleration.

With reference to water inertia time [10]:

$$T_w = \frac{Q_r}{g \cdot H_r} \cdot \sum_{i=1}^{n} \frac{L_i}{A_i} \tag{2}$$

Equation (1) becomes expressed in per unit:

$$\frac{dq}{dt} = \frac{1 - h - h_f - h_{sp}}{T_w} \tag{3}$$

In Equation (2), the water inertia time T_w includes the characteristics of all water passages with area sections A_i; corresponding lengths L_i with rated discharge Q_r; rated head H_r and gravity g. The change of water flow in the conduit is expressed in Equation (3), where h is the head at turbine; h_f is the friction head loss in the penstock and h_{sp} is the tail water head loss per unit. Water flow through the turbine [5] is given by:

$$q = G \cdot \sqrt{h} \tag{4}$$

where G is the wicket gate opening per unit of the Francis turbine and h is the head at the turbine admission per unit.

Turbine power P_m in p.u. is expressed by:

$$P_m = A_t \cdot h \cdot (q - q_{nl}) - D \cdot G \cdot \Delta w \tag{5}$$

where Δw is the speed deviation; D is the damping factor and q_{nl} is defined as no-load turbine flow. Proportionality factor A_t as described in [1] is given by Equation (6):

$$A_t = \frac{P_{m,r}}{P_{g,r} \cdot h_r \cdot (q_r - q_{nl})} \tag{6}$$

where $P_{m,r}$ is the maximum turbine rated power; $P_{g,r}$ is the generator rated power; h_r is the rated head and q_r is the rated turbine flow in p.u.

With purpose of analysing dynamic responses, linearisation in the surrounding area of operating point R was made with a Taylor series procedure (considering first two elements), e.g., linearisation of the non-linear head at turbine admission h:

$$h = \frac{q^2}{G^2} = \bar{h} + (\frac{\partial h}{\partial q})_R \cdot (q - \bar{q}) + (\frac{\partial h}{\partial G})_R \cdot (G - \bar{G}) \tag{7}$$

with calculation of partial derivation and substitution of:

$$\Delta h = h - \bar{h};\ \Delta q = q - \bar{q};\ \Delta G = G - \bar{G} \tag{8}$$

We obtain linearised Equation (9):

$$\Delta h = \frac{2 \cdot \bar{h}}{\bar{q}} \cdot \Delta q - \frac{2 \cdot \bar{h}}{\bar{G}} \cdot \Delta G \tag{9}$$

The linearisation process for all relations between Equations (3) and (5) was made with the real parameters of the Francis turbine 1 on HPP Moste. According to the synchronised generator and the fixed network frequency $\Delta w = 0$ assumption, only the first part of Equation (5) will be concerned in further analysis. The transfer function between turbine power P_m and wicket gate opening G is proposed in Equation (10):

$$\frac{\Delta Pm}{\Delta G} = \frac{b_0 \cdot s + b_1}{a_0 \cdot s + a_1} \tag{10}$$

with calculated numerator coefficients:

$$b_0 = -\sqrt{\bar{h}} \cdot (\bar{q} - q_{nl}) \cdot A_t \cdot T_w \tag{11}$$

$$b_1 = \sqrt{\bar{h}} \cdot \bar{h} \cdot A_t - \sqrt{\bar{h}} \cdot A_t \cdot (\bar{q} - q_{nl}) \cdot \left(\frac{2 \cdot \bar{q} \cdot Q_r^2 \cdot (f_{p1} + f_{p4}) + 2 \cdot \bar{q} \cdot a_0 \cdot Q_r^2 + a_1 \cdot Q_r}{H_b} \right) \quad (12)$$

and denominator coefficients in Equations (13) and (14):

$$a_0 = \frac{1}{2} \cdot \frac{\bar{q}}{\bar{h}} \cdot T_w \quad (13)$$

$$a_1 = 1 + \frac{1}{2} \cdot \frac{\bar{q}}{\bar{h}} \cdot \left(\frac{2 \cdot \bar{q} \cdot Q_r^2 \cdot (f_{p1} + f_{p4}) + 2 \cdot \bar{q} \cdot a_0 \cdot Q_r^2 + a_1 \cdot Q_r}{H_b} \right) \quad (14)$$

In connection to negative numerator coefficient b_0 in Equation (11), the non-minimal phase type of dynamic system is observed. In Figure 2, the matching of the nonlinear and calculated linear models is presented with simulation results at operating point P_m = 0.3422, G = 0.4416, q = 0.431, h = 0.9524, h_f = 0.0076 and h_{sp} = 0.015, all p.u. with real ramp reference of the wicket gate opening, in comparison to real system measurement.

Figure 2. Turbine power of the non-linear model (red solid line), linearised model (blue dashed line) and the real system measurement (green dashed line).

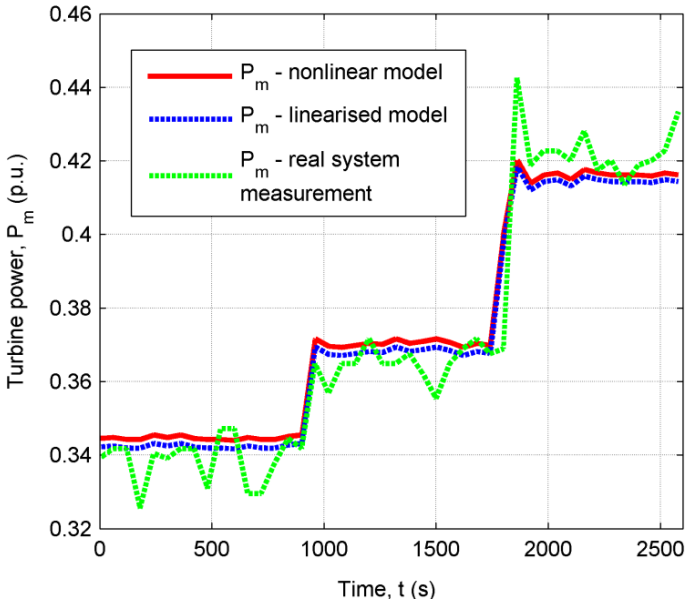

2.3. Surge Tank Modelling

In high-head HPPs, the surge tank is often included in the water system for providing the limits of water pressure fluctuation and water speed decreases in water tunnels and penstocks. There are some other important functions of surge tanks that influence the water system [18,19]: hydraulic separation of water tunnel and pressure penstock, decreasing of water hammer effect evaluation, improved results of turbine control, and acceleration of water level stabilisation.

With reference to model improvement, the surge tank with Equations (15) and (16) were included in the previously described Francis turbine model with conduit:

$$Q_s = Q_w + Q_T \quad (15)$$

where Q_s is the water flow in the tunnel; Q_w is the surge tank water flow (positive or negative) and Q_T is the turbine water flow. Water level of surge tank [1,18] is described in Equation (16):

$$\frac{dz}{dt} = \frac{Q_s - Q_T}{C_S} \tag{16}$$

with C_s expressed in Equation (17), where A_w is surge tank section area:

$$C_S = \frac{A_w \cdot h_{base}}{q_{base}} \tag{17}$$

The surge tank implemented on HPP Moste has two extended horizontal chambers with enlarged upper and bottom surface areas, A_{1_kom} and A_{3_kom}. Therefore, three different areas A_w (A_{1_kom}, A_{2_kom} and A_{3_kom}) were added to the model, depending on absolute surge tank water level calculated with relation:

$$A_w = f(z_{abs});\ z_{abs} = H_{abs} - H_{b,\max} - (z \cdot H_{b,\max}) \tag{18}$$

where H_{abs} is the nominal level of HPP water storage; $H_{b,\max}$ is the maximum available head and z_{abs} is the absolute level of surge tank.

The friction loss of head h_s and h_{fr} with friction factors f_{p2} and f_{p3} in the water tunnel are presented in Equation (19):

$$h_s = Q_s \cdot |Q_s| \cdot f_{p2}\ \ h_{fr} = f_{p3} \cdot Q_s^{\,2} \tag{19}$$

and the loss of head due to narrowed intake of the surge tank:

$$h_w = Q_w \cdot |Q_w| \cdot f_0 \tag{20}$$

where f_0 is the intake loss coefficient. The net head of surge tank is expressed in p.u. with Equation (21):

$$H_{vod} = z - h_w \tag{21}$$

which is also presented in differential Equation (22), describing flow in the water tunnel:

$$\frac{dQ_s}{dt} = \frac{H_0 - h_s - h_{fr} - H_{vod}}{T_{w1}} \tag{22}$$

and Equation (3) is modified in Equation (23):

$$\frac{dQ_T}{dt} = \frac{H_{vod} - h - h_f - h_{sp}}{T_{w2}} \tag{23}$$

where H_0 is static head of water column; T_{w1} is the water inertia time of the water passages before the surge tank intake and T_{w2} is the water inertia time between the surge tank and the Francis turbine. A dynamic system with differential Equations (16), (22) and (23) was linearised with the same Taylor series procedure as in the model without the surge tank. The third order transfer function of the HPP Moste turbine model with a conduit and surge tank was derived for three different turbine power working points: P_m = 0.3408 p.u., P_m = 0.6657 p.u. and P_m = 0.9684 p.u., with the transfer function shown in Equation (24):

$$\frac{\Delta P_m}{\Delta G} = \frac{s^3 \cdot d_0 + s^2 \cdot d_1 + s \cdot d_2 + d_3}{s^3 \cdot c_0 + s^2 \cdot c_1 + s \cdot c_2 + c_3} \tag{24}$$

Coefficients of the numerator, denominator and all other parameters in simulation are related to the real system (Francis turbine 1 HPP Moste with penstock and surge tank) and are described in Appendixes A.1. and A.2.

With the real ramp reference (slower opening rate) obtained from the HPP measurement (from 5 to 6 MW), the transient response is practically without undershot (Figure 3). With 1260 s of the simulation time, approximately ±1% of fluctuating power is presented after the reference was changed ($\Delta G = 0.0903$).

Figure 3. Dynamic response on the ramp reference of realised models at turbine power working point 0.6657 p.u.

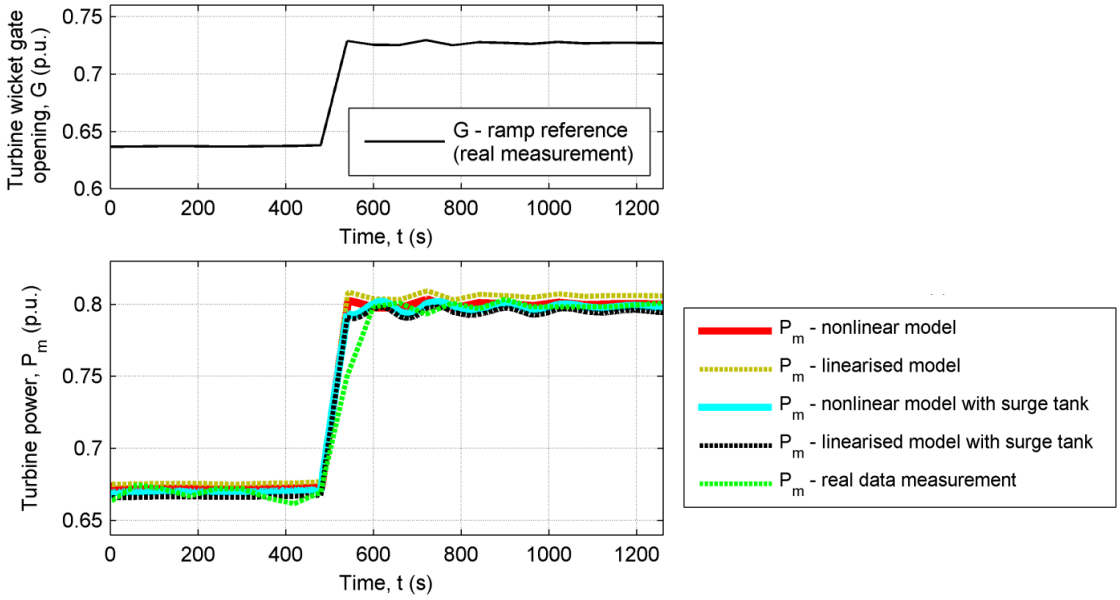

Surge tank level H_{vod} and water flow Q_w were also observed (Figure 4) during the transient response in the nonlinear model (ramp reference). The maximum difference of the water level in the surge tank was 0.0096 p.u. (0.68 m).

Figure 4. Simulated water level and water flow of the surge tank.

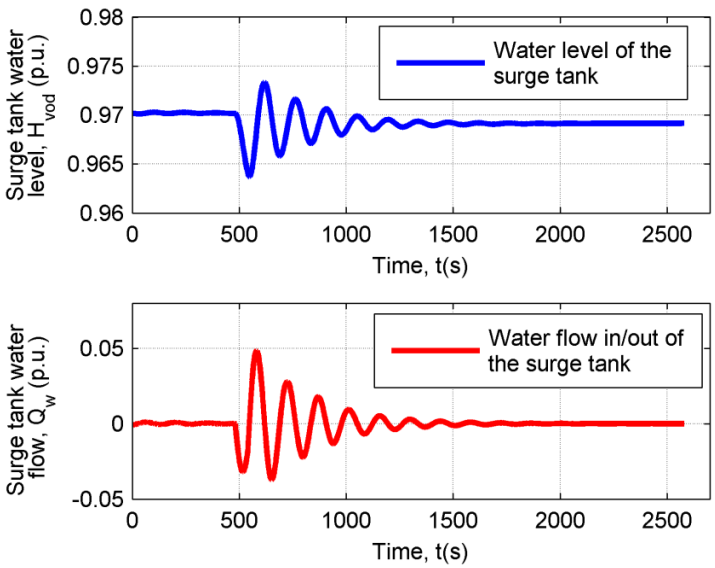

3. Fuzzy Model

In connection with the high similarity of transient responses (models with/without surge tank) depicted in Figure 3, a first order model (without surge tank) is used for fuzzy modelling. A transfer function derived from Equation (10) with time constants T_1, T_2 and gain K is presented in Equation (25):

$$G_s(s) = \frac{K \cdot (1 - T_1 \cdot s)}{1 + T_2(s)} \tag{25}$$

Due to the nonlinearity of the process, a fuzzy model was realised to determine the parameters in the middle sections of the working points. Membership functions, describing degrees of membership for input parameter P_m and output parameters K, T_1 and T_2 are presented in Figure 5.

Figure 5. Membership functions of Francis turbine model.

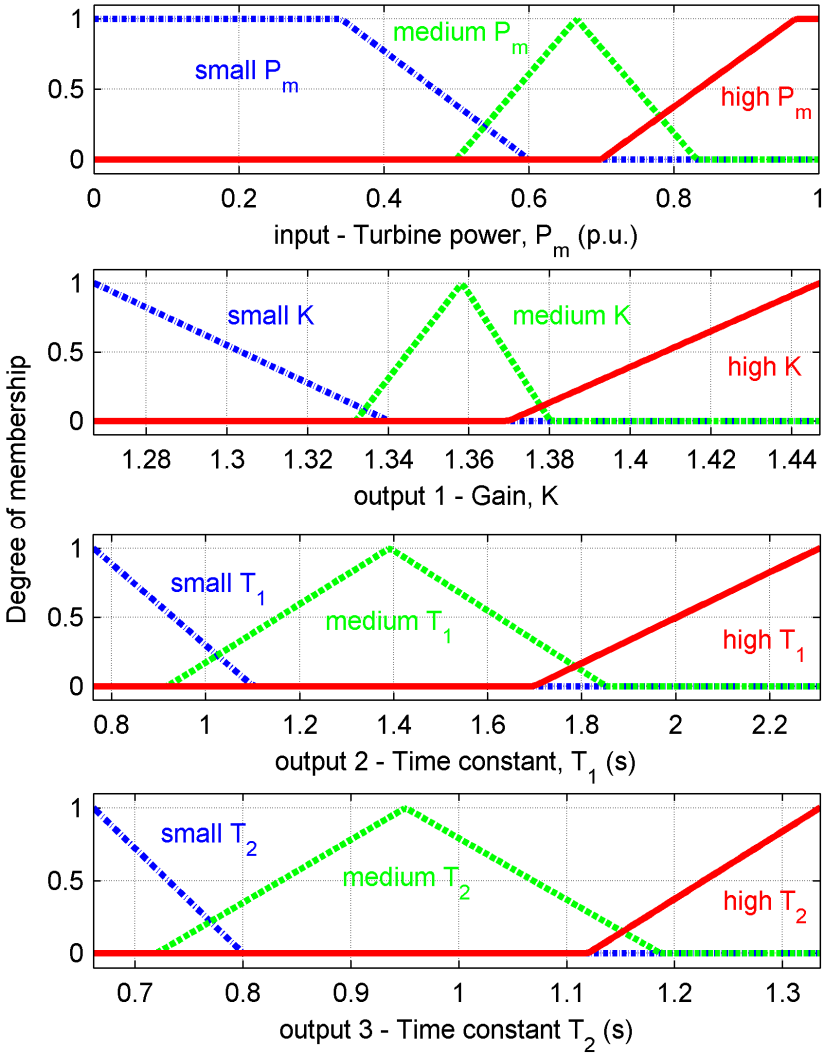

Membership functions with triangular and trapezoidal shapes were determined based on the knowledge acquired from operating experiences and intuitiveness. Fuzzy rules added to the fuzzy model are presented with rule list interpretation:

IF **turbine power P_m** = small, THEN:
- K = medium
- T_1 = small
- T_2 = small

IF **turbine power P_m** = medium, THEN:
- K = high
- T_1 = medium
- T_2 = medium

IF **turbine power P_m** = high, THEN:
- K = small
- T_1 = high
- T_2 = high

Determination of output fuzzy set was made with an aggregation method (maximum) and with a defuzzification process, where the centroid method (also called centre of area, centre of gravity) was used to obtain crisp values of parameters [20]. Turbine model parameters in working points and middle sections obtained with fuzzy model are listed in Table 1.

Table 1. Francis turbine model parameters in working points and middle sections, calculated with fuzzy model.

Turbine power	K	T_1	T_2
P_m = 0.34081	1.3583	0.7610	0.6614
P_m = 0.484	1.3565	0.8922	0.7150
P_m = 0.542	1.3935	1.2863	0.9139
P_m = 0.6657	1.4470	1.3918	0.9506
P_m = 0.7859	1.3537	1.6694	1.0515
P_m = 0.881	1.2929	2.0928	1.2593
P_m = 0.9684	1.2671	2.3073	1.3348

4. Fuzzy IMC Control and Comparison to PI Control

In connection to IMC calculation, the fuzzy model of the Francis turbine proposed in Section 3 is used. With IMC, a model is parallel-added to the process (Figure 6) and the difference between the output of the process and model is used for the feedback signal.

In an ideal case, when disturbance d = 0 and assuming the model is identical to the process, the feedback is inactive. Conversion to classic control form is made with Equation (26):

$$G_R(s) = \frac{G_{IMC}(s)}{1 - G_{IMC}(s) \cdot G_M(s)} \tag{26}$$

In the first step, the minimal phase and all-pass part of the process transfer function are expressed with Equation (27):

$$G_s(s) = \frac{K \cdot (1 - T_1 \cdot s)}{1 + T_2(s)} = \frac{K \cdot (1 + T_1(s))}{1 + T_2(s)} \cdot \frac{1 - T_1(s)}{1 + T_1(s)} \tag{27}$$

Figure 6. Internal model control.

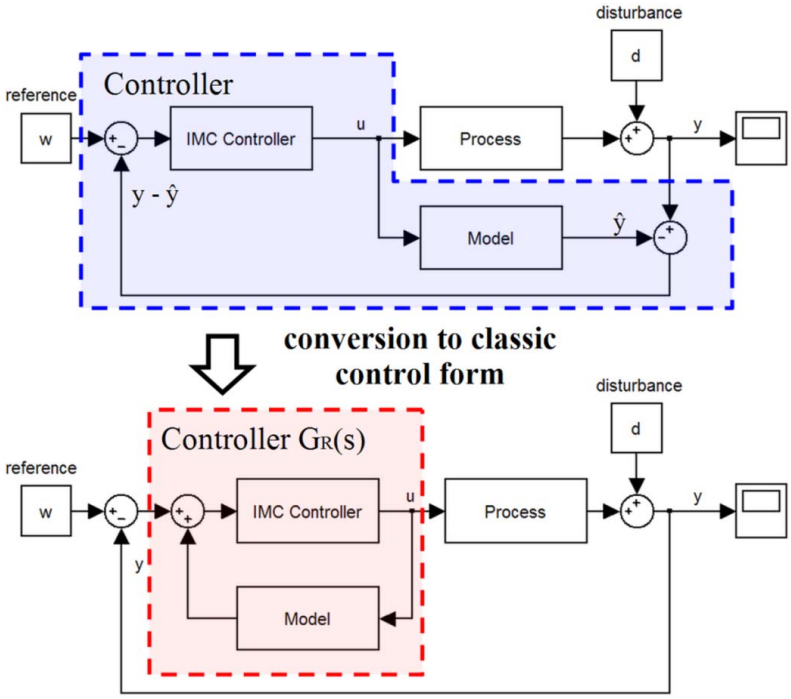

The ideal IMC controller is an inversed minimal phase part that results in mirror-transformed zeros over the ordinate axis:

$$G_{IMC}^{(opt,ideal)}(s) = \frac{1 + T_2(s)}{K \cdot (1 + T_1 \cdot s)} \tag{28}$$

Due to easier realisation and increased robustness, a PT1 (first order) filter with tuning parameter T is added to the ideal IMC controller:

$$G_{IMC}^{(opt,real)}(s) = \frac{1 + T_2(s)}{K \cdot (1 + T_1 \cdot s) \cdot (1 + T \cdot s)} \tag{29}$$

Considering Equation (26) and Figure 6, conversion to a classic controller $G_R(s)$ is expressed with Equation (30):

$$G_R(s) = \frac{1 + T_2 \cdot s}{K \cdot T \cdot T_1 \cdot s + (K \cdot T + 2 \cdot K \cdot T_1)} \cdot \frac{1}{s} \tag{30}$$

Referring to different parameters in working points from the fuzzy model, the IMC controller is presented with a matrix of transfer functions $M_R(s)$, with different tuning parameter T:

$$M_R(s) = \begin{bmatrix} G_{R1}(s); P_m = 0.34081; T = 0.3 \\ G_{R2}(s); P_m = 0.6657; T = 0.2 \\ G_{R3}(s); P_m = 0.9684; T = 0.08 \end{bmatrix} \tag{31}$$

The results of IMC with a nonlinear model and surge tank are presented in Figure 7, with 0.05 p.u. step response of turbine power and output of controller signal (wicket gate opening) in the first (G = 0.4416, P_m = 0.3408) and second working point (G = 0.6367, P_m = 0.6657). In the third working point (G = 0.9, P_m = 0.9684), a −0.05 p.u. step response was realised. The results shows a small undershoot (first and second working point) and a small overshoot at the third working point.

Figure 7. IMC control of nonlinear turbine model with conduit and surge tank for 3 different working points.

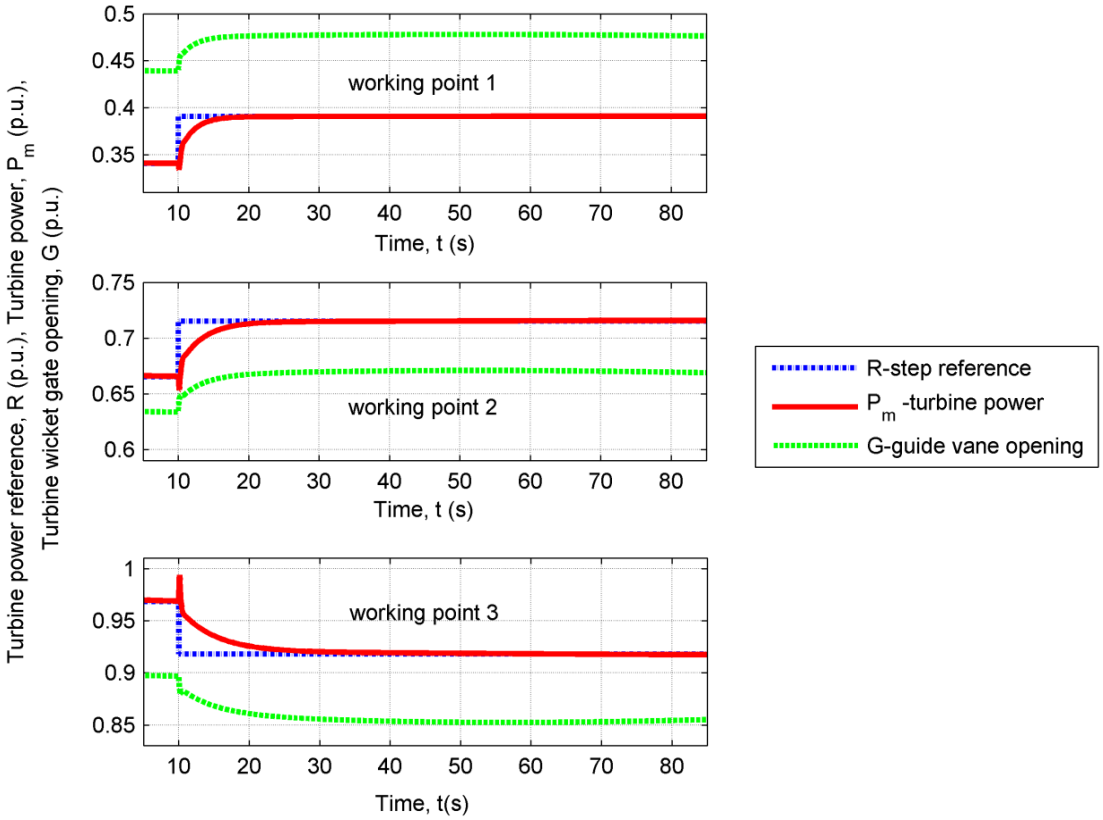

The fuzzy IMC controller algorithm was additionally formed with a fuzzy system to determine parameter T depending on turbine power P_m; while other parameters K, T_1 and T_2 are observed from a turbine fuzzy model. Results after the defuzzification process (centroid method) of tuning parameter T are presented in Table 2.

Table 2. Tuning parameter T for the internal model control (IMC) and proportional-integral (PI) parameters (K_p and K_I).

Turbine power	T (*IMC*)	K_P (*PI*)	K_I (*PI*)
$P_m = 0.34081$	0.3000	0.2983	0.3154
$P_m = 0.484$	0.2786	0.2912	0.3016
$P_m = 0.542$	0.2178	0.2709	0.2594
$P_m = 0.6657$	0.2000	0.2764	0.2437
$P_m = 0.7859$	0.1671	0.2520	0.2318
$P_m = 0.881$	0.1064	0.2329	0.1932
$P_m = 0.9684$	0.0800	0.2225	0.1759

If a hydraulic model of turbine and water passages are known, a PID or PI controller could be used for turbine power control, tuned with IAE expressed with Equation (32) or integral time absolute error (ITAE) objective function (33) with a simulation procedure [11].

$$\int |P - P_r| \cdot dt = \min \tag{32}$$

$$\int t \cdot |P - P_r| \cdot dt = \min \tag{33}$$

In Equations (32) and (33), P_r is the reference power and P is the actual power output. In connection to the IMC result validation, a PI controller with the same model was proposed. The tuning process was made with the IAE objective function, expressed with Equation (32), and tested in the same working points as the fuzzy IMC controller. A similar fuzzy system (with input—P_m, output K_p and K_I) was realised with calculated PI parameters, listed in Table 2.

Figure 8 presents turbine wicket gate opening G, turbine flow Q, head at turbine admission h; friction head loss h_f; and tail water h_{sp} for both controllers in P_m = 0.484 middle section. The influence of the PI controller proportional part fast response results in a 6% higher variation of head h at turbine admission, which consequently causes a higher under-control effect of turbine power, compared to fuzzy IMC control.

Figure 8. Wicket gate opening, turbine flow, head at turbine admission, friction head loss, and tail water in p.u. with fuzzy internal model control (IMC) and proportional-integral (PI) control in the middle section at turbine power 0.484 p.u.

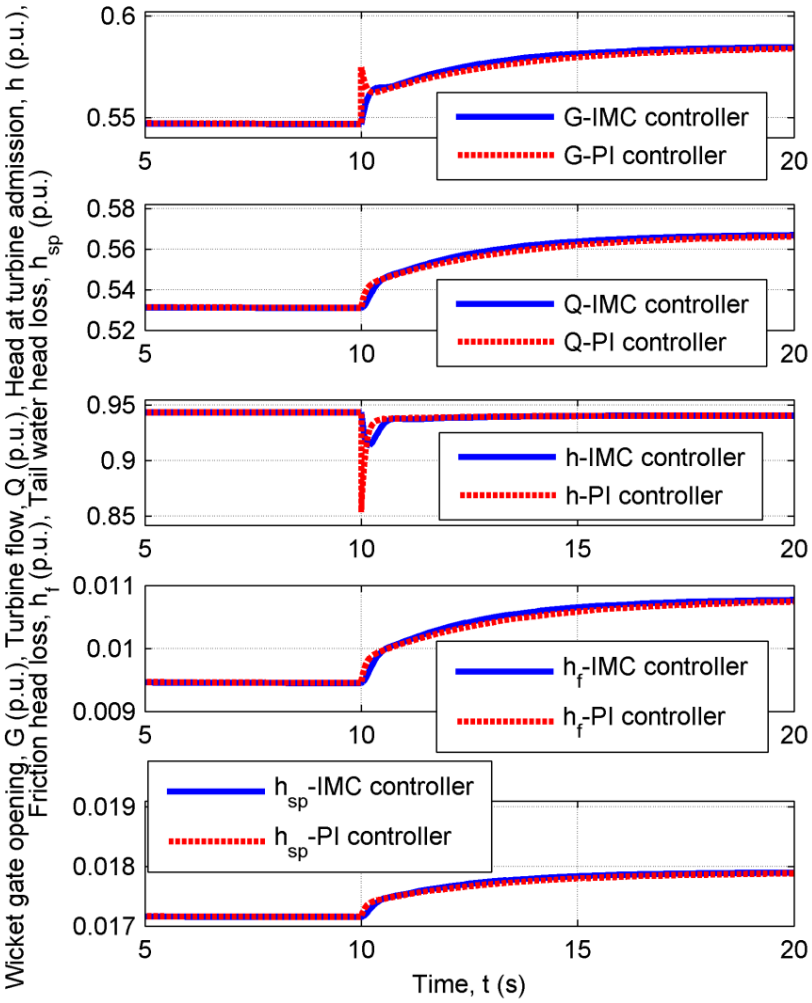

The fuzzy IMC controller in middle section P_m = 0.484 provides 0.200 p.u. undershoot M_p in comparison to 0.915 p.u. with PI controller (Figure 9). Comparison results for the four middle sections of working points are presented in Table 2 (bolded values).

Figure 9. Step response of the turbine power with fuzzy IMC and PI controller in the middle sections of working points.

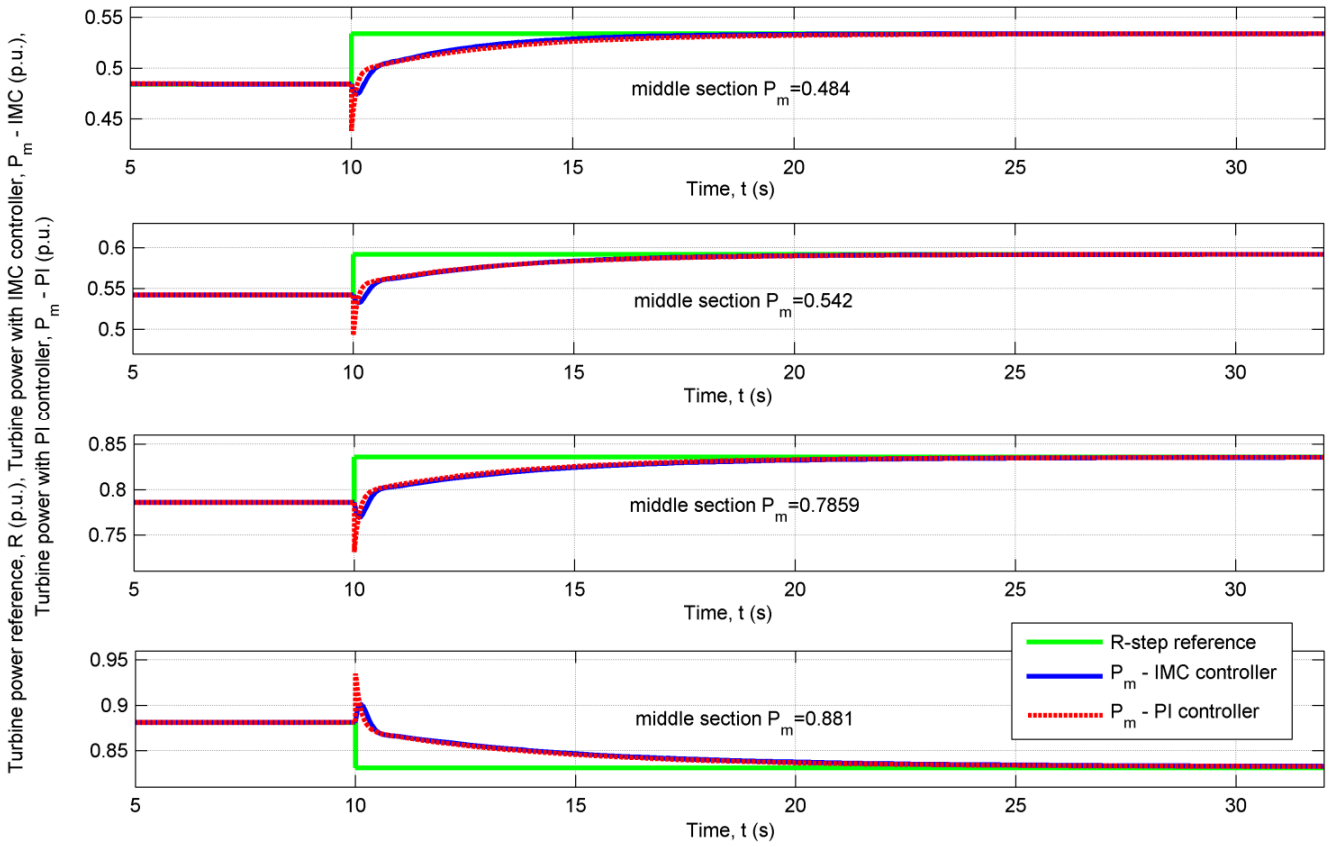

The smallest under-control power effect with 0.200 p.u. undershoot is obtained with IMC in P_m = 0.484 (Table 3); however, the highest under-control effect 1.088 p.u. is observed at P_m = 0.7859 with PI controller. Turbine head drop Δh has the smallest value 0.020 p.u. with the IMC controller in P_m = 0.881; and the highest value 0.086 p.u. with the PI controller in P_m = 0.484 middle section.

Table 3. Turbine maximum undershoot M_p and head drop Δh at turbine admission with fuzzy IMC and PI control.

Comparison IMC/PI control	P_m **= 0.484**	P_m **= 0.542**	P_m **= 0.7859**	P_m **= 0.881**
M_p IMC (p.u.)	0.200	0.202	0.340	0.410
M_p PI (p.u.)	0.915	0.990	1.088	1.076
Δh IMC (p.u.)	0.027	0.022	0.022	0.020
Δh PI (p.u.)	0.086	0.083	0.061	0.050

In comparison to the PI controller, fuzzy IMC presents better results, with lower undershoots M_p in all four middle sections and with approximately the same settle time on the step reference of turbine power P_m.

Fuzzy IMC also provides smaller variations of head Δh at turbine admission, which ensures fewer oscillations of the HPP water system.

5. Conclusions

In this paper, the dynamic modelling of a Francis turbine 1 (HPP Moste) with and without a surge tank with linearisation and IMC power control was proposed. With the actual HPP technical data (water tunnels and conduits), the presented models show a good match to the real data measurement.

With linearisation, a first-order transfer function with non-minimal phase was used for fuzzy modelling. Concerning appropriately defined input and output membership functions, a fuzzy rule list and the defuzzification process (centroid method), the crisp parameters of the Francis turbine model were calculated.

Based on the fuzzy model, a fuzzy IMC controller was proposed with calculation of tuning parameter T, depending on turbine power. For IMC validation, the PI controller with IAE objective function and fuzzy inference system (similar to IMC) was proposed. A comparison of the fuzzy IMC and PI control with maximum undershoot M_p and head variations Δh criterion in the middle sections of working points shows that IMC has better results due to the smaller undershoot on step response, smaller head variations Δh and easier tuning process (one tuning parameter T) in case of acquired model.

The applied methodology with the extension of working points with different static heads can be used as algorithm in digital turbine governor in order to ensure better results in water turbine power control.

Conflicts of Interest

The authors declare no conflict of interest.

Appendix

A1. Numerator and Denominator Coefficients of Transfer Function Presented in Section 2.3. (24)

$$d_0 = -\sqrt{h} \cdot (\overline{Q} \cdot A_T - q_{nl} \cdot A_T) \cdot T_{w1} \cdot T_{w2} \cdot H_b \cdot C_s \tag{A1}$$

$$d_1 = -\sqrt{h} \cdot (\overline{Q} \cdot A_T - q_{nl} \cdot A_T) \cdot (C_s \cdot T_{w1} \cdot (2 \cdot \overline{Q} \cdot Q_r^2 \cdot f_{p1} + 2 \cdot \overline{Q} \cdot a_0 \cdot Q_r^2 + a_1 \cdot Q_r) + 2 \cdot T_{w2} \cdot f_{p3} \cdot \overline{Q_s} \cdot H_b \cdot C_s) + \sqrt{\overline{h}} \cdot \overline{h} \cdot A_t \cdot H_b \cdot C_s \cdot T_{w1} \tag{A2}$$

$$d_2 = -\sqrt{h} \cdot (\overline{Q} \cdot A_T - q_{nl} \cdot A_T) \cdot (H_b \cdot (T_{w1} + T_{w2}) + 2 \cdot f_{p3} \cdot \overline{Q_s} \cdot C_s \cdot (2 \cdot \overline{Q} \cdot Q_r^2 \cdot f_{p1} + 2 \cdot \overline{Q} \cdot a_0 \cdot Q_r^2 + a_1 \cdot Q_r)) + 2 \cdot \sqrt{\overline{h}} \cdot \overline{h} \cdot A_t \cdot f_{p3} \cdot H_b \cdot C_s \cdot \overline{Q_s} \tag{A3}$$

$$d_3 = -\sqrt{h} \cdot (\overline{Q} \cdot A_T - q_{nl} \cdot A_T) \cdot (2 \cdot \overline{Q} \cdot Q_r^2 \cdot f_{p1} + 2 \cdot \overline{Q} \cdot a_0 \cdot Q_r^2 + a_1 \cdot Q_r + 2 \cdot f_{p3} \cdot \overline{Q_s} \cdot H_b) + \sqrt{\overline{h}} \cdot \overline{h} \cdot A_t \cdot H_b \tag{A4}$$

$$c_0 = \frac{1}{2} \cdot \frac{\overline{Q}}{\overline{h}} \cdot T_{w1} \cdot T_{w2} \cdot H_b \cdot C_s \tag{A5}$$

$$c_1 = \frac{1}{2} \cdot \frac{\overline{Q}}{\overline{h}} \cdot (C_s \cdot T_{w1} \cdot (2 \cdot \overline{Q} \cdot Q_r^2 \cdot f_{p1} + 2 \cdot \overline{Q} \cdot a_0 \cdot Q_r^2 + a_1 \cdot Q_r) + 2 \cdot T_{w2} \cdot f_{p3} \cdot \overline{Q_s} \cdot H_b \cdot C_s) H_b \cdot C_s \cdot T_{w1} \tag{A6}$$

$$c_2 = \frac{1}{2}\cdot\frac{\overline{Q}}{\overline{h}}\cdot(H_b\cdot(T_{w1}+T_{w2})+2\cdot f_{p3}\cdot\overline{Q_s}\cdot C_s\cdot(2\cdot\overline{Q}\cdot Q_r{}^2\cdot f_{p1}+2\cdot\overline{Q}\cdot a_0\cdot Q_r{}^2+a_1\cdot Q_r)+ 2\cdot f_{p3}\cdot\overline{Q_s}\cdot H_b\cdot C_s \quad \text{(A7)}$$

$$c_3 = \frac{1}{2}\cdot\frac{\overline{Q}}{\overline{h}}\cdot(2\cdot\overline{Q}\cdot Q_r^2\cdot f_{p1}+2\cdot\overline{Q}\cdot a_0\cdot Q_r^2+a_1\cdot Q_r+2\cdot f_{p3}\cdot\overline{Q_s}\cdot H_b)+H_b \quad \text{(A8)}$$

A2. Model Parameters

Table A1. Model parameters.

Parameter	Symbol	Value
Generator rated power	$P_{g,r}$	9 MVA
Maximum turbine rated power	$P_{m,r}$	7.5 MW
Rated turbine power	P_r	6.692 MW
Maximum turbine flow	$Q_{\max}$	14 m^3/s
Rated turbine flow	Q_r	13 m^3/s
No-load flow	q_{nl}	0.19 p.u.
Rated turbine head p.u.	h_r	0.824 p.u.
Static head p.u.	h_0	0.9740 p.u.
Static head	h_b	68.62 m
Gravity constant	g	9.80665 m/s^2
Water inertia time	T_{w1}	2.2361 s
Water inertia time	T_{w2}	0.7267 s
Water inertia time	T_{w3}	2.9628 s
Surge tank intake loss	f_0	0.0005
Friction loss penstock	f_{p1}	0.0136
Friction loss water tunnel	f_{p2}	0.0136
Additional friction loss of the water tunnel	f_{p3}	0.01
Additional friction loss of the penstock	f_{p4}	0.003
Surge tank parameter	C_s	225.5150 s
Turbine damping	D	0.5 p.u./p.u.
Surge tank upper chamber area	$A1\_kom$	316.6 m^2
Surge tank main chamber area	$A2\_kom$	44.2 m^2
Surge tank bottom chamber area	$A3\_kom$	276.4 m^2

References

1. De Mello, F.P.; Koessler, R.J.; Agee, J.; Anderson, P.M.; Doudna, J.H.; Fish, J.H., III; Hamm, P.A.L.; Kundur, P.; Lee, D.C.; Rogers, G.J.; *et al*. Hydraulic turbine and turbine control models for system dynamic studies. *IEEE Trans. Power Syst.* **1992**, *7*, 167–179.
2. De Jaeger, E.; Janssens, N.; Malfliet, B.; van de Meulebroeke, F. Hydro turbine model for system dynamic studies. *IEEE Trans. Power Syst.* **1994**, *9*, 1709–1715.
3. Ng, T.B.; Walker, G.J.; Sargison, J.E. Modelling of Transient Behaviour in a Francis Turbine Power Plant. In Proceedings of the 15th Australasian Fluid Mechanics Conference, Sydney, Australia, 13–17 December 2004.

4. Fraile-Ardanuy, J.; Wilhelmi, J.R.; Fraile-Mora, J.; Pérez, J.I.; Sarasua, I. A Dynamic Model of Adjustable Speed Hydro Plants. In Proceedings of the 9th Congreso Hispano Luso de Ingeniería Eléctrica, Marbella, Spain, 30 June–2 July 2005.
5. Hannett, L.N.; Feltes, J.W.; Fardanesh, B. Field tests to validate hydro turbine-governor model structure and parameters. *IEEE Trans. Power Syst.* **1994**, *9*, 1744–1751.
6. Němec, Z.; Němec, V. Water turbine power control feasible conception. *Eng. Mech.* **2009**, *16*, 403–411.
7. Win, T.N. Hydraulic Governor Control System for Francis Turbine. In Proceedings of at the GMSARN International Conference on Sustainable Development: Issues and Prospects for the GMS, Kunming, China, 12–14 November 2008.
8. Chen, D.; Ding, C.; Ma, X.; Yuan P.; Ba, D. Nonlinear dynamical analysis of hydro-turbine governing system with a surge tank. *Appl. Math. Model.* **2013**, *37*, 7611–7623.
9. Li, W.; Vanfretti, L.; Chompoobutrgool, Y. Development and implementation of hydro turbine and governor models in a free and open source software package. *Simul. Model. Pract. Theory* **2012**, *24*, 84–102.
10. International Electrotechnical Committee (IEC). *IEC 60308: Hydraulic Turbines—Testing of Control Systems*, 2nd ed.; IEC: Geneva, Switzerland, 2005.
11. International Electrotechnical Committee (IEC). *IEC 61362: Guide to Specification of Hydraulic Turbine Control Systems*, 1st ed.; IEC: Geneva, Switzerland, 1998.
12. Mahmoud, M.; Dutton, K.; Denman, M. Design and simulation of a nonlinear fuzzy controller for a hydropower plant. *Electr. Power Syst. Res.* **2005**, *73*, 87–99.
13. Tan, W. Unified tuning of PID load frequency controller for power systems via IMC. *IEEE Trans. Power Syst.* **2010**, *25*, 341–350.
14. Chen, Z.; Yuan, X.; Tian, H.; Ji, B. Improved gravitational search algorithm for parameter identification of water turbine regulation system. *Energy Convers. Manag.* **2014**, *78*, 306–315.
15. Fang, H.; Chen, L.; Shen, Z. Application of an improved PSO algorithm to optimal tuning of PID gains for water turbine governor. *Energy Convers. Manag.* **2011**, *52*, 1763–1770.
16. Naik, K.A.; Srikanth, P.; Negi, P. IMC tuned PID governor controller for hydro power plant with water hammer effect. *Procedia Technol.* **2012**, *4*, 845–853.
17. Hušek, P. PID controller design for hydraulic turbine based on sensitivity margin specifications. *Int. J. Electr. Power Syst.* **2014**, *55*, 460–466.
18. Giesecke, J.; Mosonyi, E. *Wasserkraftanlagen: Planung, Bau und Betrieb*, 2nd ed.; Springer: Berlin, Germany, 1998; pp. 293–305.
19. Mosonyi, E. *Water Power Development: High-Head Power Plants*, 3rd ed.; Akadémiai Kiadó: Budapest, Hungary, 1991; Volume 2/B, pp. 975–985.
20. Ross, T.J. *Fuzzy Logic with Engineering Applications*, 2nd ed.; John Wiley & Sons: Chichester, UK, 2004; p. 101.